International Journal of Engineering, Mathematical and Physical Sciences
ISSN: 2517-9934
Vol:5, No:9, 2011

Transonic Flutter Analysis Using Euler Equation and Reduced Order Modeling Technique

D. H. Kim, Y. H. Kim, and T. Kim

***Abstract*—**A new method identifies coupled fluid-structure system with a reduced set of state variables is presented. Assuming that the structural model is known a priori either from an analysis or a test and using linear transformations between structural and aeroelastic states, it is possible to deduce aerodynamic information from sampled time histories of the aeroelastic system. More specifically given a finite set of structural modes the method extracts generalized aerodynamic force matrix corresponding to these mode shapes. Once the aerodynamic forces are known, an aeroelastic reduced-order model can be constructed in discrete-time, state-space format by coupling the structural model and the aerodynamic system. The resulting reduced-order model is suitable for constant Mach, varying density analysis.

***Keywords*—**ROM (Reduced-Order Model), Aeroelasticity, AGARD 445.6 wing,

NOMENCLATURE

$\mathbf{A}$ $\mathbf{B}$ $\mathbf{C}$	Structural system matrices
$\mathbf{A}_a$ $\mathbf{B}_a$ $\mathbf{C}_a$ $\mathbf{D}_a$	Aerodynamic system matrices
$\mathbf{A}_t$ $\mathbf{B}_t$ $\mathbf{C}_t$	Aeroelastic system matrices
$\mathbf{A}_{ta}$	Aerodynamic sub-matrix defied in (27)
$\mathbf{C}_{ta}$	Aerodynamic output sub-matrix defined in (32)
$\mathbf{C}_v$	Aeroelastic output matrix for aerodynamic measurements
$\mathbf{C}_w$	Aeroelastic output matrix for structural measurements
$\mathbf{F}$	Forcing input matrix for structure
$\mathbf{G}$	Generalized damping matrix
$\mathbf{K}$	Generalized stiffness matrix
$\mathbf{M}$	Generalized mass matrix
Mach	Mach number
M	Number of time steps
N	Number of structural modes or displacement measurements
na	Number of aerodynamic measurements
$\mathbf{P}$	($2N \times 1$) generalized coordinates vector
Q_{ij}	Generalized aerodynamic force coefficients
q	Dynamic pressure ($\equiv \frac{1}{2}\rho V^2$)
q_{ref}	Reference dynamic pressure at which aeroelastic responses are sampled
R	Dimension of structural states vector $\mathbf{x}$
Re	Reynolds number
R_t	Dimension of aeroelastic states vector $\mathbf{Y}$
$\mathbf{T}_\eta$	Transformation matrix from x to $\mathbf{Y}_x$
$\mathbf{T}_\zeta$	Transformation matrix from $\mathbf{Y}$ to $\mathbf{x}$
t	Real time
$\mathbf{u}$	control inputs vector
$U \sum V$	Singular value decomposition matrices
V	Free stream air speed
V_{ref}	Reference air speed at which aeroelastic responses are sampled
$\mathbf{v}$	($na \times 1$) aerodynamic measurements vector
$\mathbf{w}$	($2N \times 1$) structural measurements vector ($\equiv \begin{Bmatrix} \mathbf{z} \\ \dot{\mathbf{z}} \end{Bmatrix}$)
$\mathbf{x}$	($R \times 1$) structural states vector
$\mathbf{y}$	Aerodynamic states vector
$\mathbf{Y}$	($R_t \times 1$) aeroelastic states vector
$\mathbf{Y}_x$	($R_t \times 1$) structural sub-states vector
$\mathbf{Y}_y$	($R_t \times 1$) aerodynamic sub-states vector
$\mathbf{z}$	($N \times 1$) displacement measurements vector
Φ	Structural sensor matrix
ρ	Air density

D. H. Kim is with Gyeongsang National University (GNU), Jinju City, Gyungnam, Republic of Korea (phone: 82+55-755-2083; fax: 82+55-755-2083; e-mail: dhk@gnu.ac.kr).

Y. H. Kim is with Gyeongsang National University (GNU), Jinju City, Gyungnam, Republic of Korea (e-mail: kyh@gnu.ac.kr).

T. Kim is with the Gyeongsang National University (GNU), Jinju City, Gyungnam, Republic of Korea (e-mail: txkim @ comcast.net).

I. INTRODUCTION

IN the past much effort has been made to utilize advanced Computational Fluid Dynamic (CFD) programs for aeroelastic simulations and analyses of military and civil aircraft. However, although the use of CFD is quite broad for static aerodynamic and aeroelastic calculations nowadays, it is limited in the field of unsteady aeroelasticity due to enormous size of computer memory and unreasonably long CPU time associated with long time periods required to observe transient responses and a large number structural modes. While a military airplane model may need 20-50 modes, a commercial aircraft model typically includes as many as 200 modes to describe the motion of the structure with enough accuracy. Thus, much research has been conducted on model reduction of the coupled fluid-structure systems including the eigen analysis [1]-[2], the Proper Orthogonal Decomposition (POD) or Karhunen-Loeve (KL) method [3]-[6], system identification methods [7]-[10]. However, in all of the methods the aerodynamics is treated separately from the structure making them difficult and inconvenient for structural engineers to apply.

Recently, Kim [11], [12] developed a novel system identification and model reduction technique, also known as "Aerodynamics is Aeroelasticity minus Structure" (AAEMS),

for linear time-invariant, coupled fluid-structure systems. Unlike the previous methods, it works directly on time history data of the coupled aeroelastic system. Assuming that structural properties are known a priori, and using linear transformations between the structural and aeroelastic states, it extracts and models the underlying aerodynamic system with a finite number of state variables. Using two types of CSD/CFD models and simulations, Kim showed that the method is able to produce aerodynamic and aeroelastic ROMs with high accuracy without requiring a long CPU time normally associated with a large number of structural modes.

In this paper, to demonstrate further the efficiency and accuracy of the new model reduction method, we will examine AGARD 445.6 wing modeled by FLUENT CFD and NASTRAN FEM programs. See Fig. 1 and Table I for the finite element model and its specifications. The wing motion is described by four natural modes and their natural frequencies are listed in Table II. Aeroelastic responses of the coupled CSD/CFD system, i.e., the displacements and velocities of the four structural coordinates will be recorded in time. In addition, unsteady pressures will be calculated at various points on the wing during the numerical simulation. These aerodynamic samples are necessary to generate aerodynamic ROM that is valid for all dynamic pressure values. All the responses will be obtained for a fixed Mach, at a low sub-critical dynamic pressure value. Once the aerodynamic ROM is obtained, an aeroelastic ROM can be constructed by coupling the aerodynamic ROM with the structural model. Using the ROM one can predict flutter by making Vg plot as a function of the dynamic pressure. It is also possible to use the model for other aeroelastic analyses such as dynamic flight loads and active control design. See Ref. [11-12] for examples of Vg plots obtained by the AAEMS and the aeroelastic ROM.

Since the AGARD wing does not have any control surface, it is necessary to make up an artificial input for the purpose of the system identification. For example, any (8x1) arbitrary vector array with zeros in the top four and non-zeros in the bottom four entries multiplied by an impulse or a random time function will fulfill the requirement. More conveniently, however, an initial condition in the velocity components of the four structural coordinates can be imposed and the corresponding aeroelastic responses can be obtained.

It is expected that the accuracy of the aeroelastic ROM will largely depend on the number and locations of the aerodynamic pressures. Kim [12] showed previously that even without the pressure data the AAEMS will accurately predict aeroelastic behavior in the neighborhood of the reference dynamic pressure. It was also shown that in order to improve the accuracy and extend its range away from the reference point it is necessary to add a sufficient number of the aerodynamic measurements. What is not known is optimum locations of the pressure points that will lead to an optimal aeroelastic ROM and this will be the main focus of the proposed research. Thus, different combinations of pressure values at different locations will be tested and the results will be reported in the final paper.

Finally, advantages of using the new model reduction method over traditional methods will be discussed. More specifically, it is expected that the CPU time required for sampling the aeroelastic responses and creating the ROM will be significantly reduced. This is because in the new method there is no need to execute the mode-by-mode excitation for the calculation of the generalized aerodynamic force (GAF) matrix. In the case of the AGARD wing modeled by four natural modes, a single set of time samples due to a single initial condition will be sufficient to generate accurate ROM and therefore the saving in the computing time will be nearly a factor of four. An equally important advantage is that for structural engineers it will make the process of generating aerodynamic ROM handy and convenient because it bypasses the necessity to deal with the CFD directly.

II. COMPUTATIONAL BACKGROUNDS

A. Basic Assumption

We will assume that time histories of airplane structural and aerodynamic responses due to certain inputs, e.g., control surfaces, are available at both zero and nonzero air speeds. The structural responses here are displacements and velocities at various positions on the airplane, whereas the aerodynamic responses could be pressure measurements (in the case of tests, specially), or in the case of numerical simulations any of the independent aerodynamic variables such as vorticities, potentials in the flow field.

The following assumptions are also made.

1. Structure, aerodynamics, and aeroelasticity are all dynamically linear, i.e., have small perturbed oscillations.
2. The airplane is flying along a CMVD curve.
3. Sufficient numbers of structural and aeroelastic measurements are available.
4. Background noise in the data is minimal or has been subdued by standard signal processing.
5. The system is controllable and observable.

Fig.2.1 represent the process to develop ROM system using AAEMS (Aerodynamics is Aeroelasticity minus Structure) method. There are two way to predict flutter boundary (see Fig 2.2). One is CMVD (Constant Mach, Varying Density) and the other is CDVM (Constant Density, Varying Mach). CMVD is the method that predicts flutter boundary according to various flight altitudes with constant Mach and CDVM is the method according to various Mach with constant flight altitude. CDVM method is used in this study.

B. Structural and Aerodynamic measurement

First, at M time steps $t = 0, \Delta t, 2\Delta t, \cdots, (M-1)\Delta t$ we take airplane responses on the ground and in the air:

$$[\mathbf{w}^0 \quad \mathbf{w}^1 \quad \mathbf{w}^2 \quad \cdots \quad \mathbf{w}^{\mathbf{M}-1}] \,@\, V = 0 \tag{1}$$

$$\begin{bmatrix} \mathbf{v}^0 & \mathbf{v}^1 & \mathbf{v}^2 & \cdots & \mathbf{v}^{\mathbf{M}-1} \\ \mathbf{w}^0 & \mathbf{w}^1 & \mathbf{w}^2 & \cdots & \mathbf{w}^{\mathbf{M}-1} \end{bmatrix} @\, V = V_{ref} \tag{2}$$

These time samples represent the structural dynamic and aeroelastic systems respectively, and could be obtained from

either Computational Structural Dynamics (CSD)/(CFD) simulations, or from GVT/WTT or FFT (See Fig 2.3).

Once we have collected the time history samples we can identify the system output matrices using a standard data processing. For instance, the Singular Value Decomposition (SVD) produces:

$$[\mathbf{w}^0 \quad \mathbf{w}^1 \quad \mathbf{w}^2 \quad \cdots \quad \mathbf{w}^{M-1}]_{V=0} \cong \mathbf{U}_R \Sigma_R^{1/2} \cdot \Sigma_R^{1/2} \mathbf{V}_R^T \equiv \mathbf{C}\left[\mathbf{x}^0 \mathbf{x}^1 \mathbf{x}^2 \cdots \mathbf{x}^{M-1}\right] \quad (3)$$

$$\begin{bmatrix} \mathbf{v}^0 & \mathbf{v}^1 & \mathbf{v}^2 & \cdots & \mathbf{v}^{M-1} \\ \mathbf{w}^0 & \mathbf{w}^1 & \mathbf{w}^2 & \cdots & \mathbf{w}^{M-1} \end{bmatrix}_{V=V_{ref}} \cong \mathbf{U}_{Rt} \Sigma_{Rt}^{1/2} \cdot \Sigma_{Rt}^{1/2} \mathbf{V}_{Rt}^T \equiv \mathbf{C}_t \left[\mathbf{Y}^0 \mathbf{Y}^1 \mathbf{Y}^2 \cdots \mathbf{Y}^{M-1}\right] \quad (4)$$

where

$$\mathbf{C}_t = \begin{bmatrix} \mathbf{C}_\upsilon \\ \mathbf{C}_\varpi \end{bmatrix} \quad (5)$$

Note that the realization by the SVD guarantees the matrices with minimum sizes. That is, R and R_t are the ranks of the data covariance matrices with the structural and aeroelastic time samples, respectively.

C. Topology and Transformation of states

Within the aeroelastic system one can split the aeroelastic states Y into the structural part $\mathbf{Y_x}$ and the aerodynamic part $\mathbf{Y_y}$. The dimension of the sub-state vectors is R_t but they are rank deficient, i.e., have ranks smaller than R_t (see Fig 2.4 for topological description)

Since both the structural and aeroelastic samples have the common structural measurement w, it is possible to relate between **x**, **Y**, and $\mathbf{Y_x}$ through transformation matrices. Towards this end, we will assume that during the flight the structure behaves the same way as it was described by CSD or GVT. That is, the output matrix C relating the structural states and the responses still satisfies (3) except that x now represents the structural states within the aeroelastic system. The equation (3) and the structural portion of (4) yields

$$\mathbf{x} = \mathbf{T}_\zeta \mathbf{Y} \quad (6)$$

$$\mathbf{Y_x} = \mathbf{T}_\eta \mathbf{x} \quad (7)$$

Where

$$\mathbf{T}_\eta \equiv \mathbf{C}_{t2}^{-\mathbf{p}} \mathbf{C} \quad (8)$$

$$\mathbf{T}_\zeta \equiv \mathbf{C}^{-\mathbf{p}} \mathbf{C}_\mathbf{w} \quad (9)$$

$$\mathbf{I} = \mathbf{T}_\zeta \mathbf{T}_\eta \quad (10)$$

And

$$\mathbf{C}_{t2}^{-\mathbf{p}} \equiv \textit{the last 2N colums of } \mathbf{C}_\mathbf{t}^{-\mathbf{p}} \quad (11)$$

Here, $(\ )^{-p}$ denotes pseudo-inversion of matrix

Relation between x, Y, and $\mathbf{Y}_x$

Since **v** and **w** contain only the aerodynamic and structural data, respectively, $\mathbf{Y}_x$ and $\mathbf{Y}_y$ are additive and complementary satisfying the following property:

$$\mathbf{Y} = \mathbf{Y_x} + \mathbf{Y_y} = \mathbf{f_x}(\mathbf{Y}) + \mathbf{f_y}(\mathbf{Y}) \quad (12)$$

Where $\mathbf{f}_x$ and $\mathbf{f}_y$ represent mappings from the aeroelastic states to the structural and aerodynamic sub-states:

$$\mathbf{f_x} \equiv \mathbf{T}_\eta \mathbf{T}_\zeta \quad (13)$$

$$\mathbf{f_x} \equiv \mathbf{I} - \mathbf{T}_\eta \mathbf{T}_\zeta \quad (14)$$

Additional properties of $\mathbf{f}_x$, $\mathbf{f}_y$

It can be shown that $\mathbf{f}_x$ and $\mathbf{f}_y$ themselves are also complementary and hence satisfy

$$\mathbf{f_x}(\mathbf{f_y}) = 0 \quad (15)$$

$$\mathbf{f_y}(\mathbf{f_x}) = 0 \quad (16)$$

Said another way, “structural mapping on aerodynamics and aerodynamic mapping on structure produce zeros.”

Also,

$$\mathbf{f_x}(\mathbf{f_x}) = \mathbf{f_x} \quad (17)$$

$$\mathbf{f_y}(\mathbf{f_y}) = \mathbf{f_y} \quad (18)$$

That is, “Structural mapping on structure and aerodynamic mapping on aerodynamics produce themselves.”

D. Structural and Aeroelastic Systems in Time Domain

Along with the identification of the output matrices and states, full realizations of the structural and aeroelastic systems can be obtained in discrete-time, state-space format using standard system identification methods such as ERA (Eigensystem Realization Algorithm), ARMA (Auto Regressive Moving Average), OKID (Observer kalman Filter Identification), SCI/ERA ingle-composite-Input/ERA), etc.-

Structure

$$\mathbf{x}^{\mathbf{n}+1} = \mathbf{A}\mathbf{x}^{\mathbf{n}} + \mathbf{B}\mathbf{u}^{\mathbf{n}} \tag{19}$$

$$\mathbf{w}^{\mathbf{n}} = \mathbf{C}\mathbf{x}^{\mathbf{n}} \tag{20}$$

Aeroelasticity

$$\mathbf{Y}^{\mathbf{n}+1} = \mathbf{A}_{\mathbf{t}}\mathbf{Y}^{\mathbf{n}} + \mathbf{B}_{\mathbf{t}}\mathbf{u}^{\mathbf{n}} \tag{21}$$

$$\begin{Bmatrix}\mathbf{v}^{\mathbf{n}}\\ \mathbf{w}^{\mathbf{n}}\end{Bmatrix} = \mathbf{C}_{\mathbf{t}}\mathbf{Y}^{\mathbf{n}} = \begin{bmatrix}\mathbf{C}_{\mathbf{v}}\\ \mathbf{C}_{\varpi}\end{bmatrix}\mathbf{Y}^{\mathbf{n}} \tag{22}$$

It must be mentioned that the structural model could be also obtained directly from a Finite Element Method (FEM) in which the structural equations of motion are expressed in terms of a finite number of mode shapes. If desired, the computational model can be updated based on the GVT data. In this case, the structural mass, damping, stiffness, and forcing matrices will be available to construct an equation of motion in continuous time,

$$\mathbf{M}\ddot{\mathbf{p}} + \mathbf{G}\dot{\mathbf{p}} + \mathbf{K}\mathbf{p} = \mathbf{F}\mathbf{u} \tag{23}$$

Form which (19) and (20) can be obtained by discretizing the time derivatives with the incremental time step dt. Note that the structural states in this case are the modal displacements and modal velocities, i.e., $\mathbf{x} \equiv [\mathbf{p}\dot{\mathbf{p}}]^{\mathbf{T}}$,and

$$\mathbf{z} = \Phi\mathbf{p} \tag{24}$$

where Φ is a sensor matrix that transforms the modal coordinates to the physical displacements.

E. Identification of Aerodynamic System

Differential equations for the aerodynamics can be found by subtracting the structural sub-states from the aeroelastic states:

$$\mathbf{Y}_{\mathbf{y}}{}^{\mathbf{n}+1} = \mathbf{Y}^{\mathbf{n}+1} - \mathbf{Y}_{\mathbf{x}}{}^{\mathbf{n}+1} \tag{25}$$

which, after using (7) and (21), becomes

$$\mathbf{Y}_{\mathbf{y}}{}^{\mathbf{n}+1} = \mathbf{A}_{\mathbf{t}}[\mathbf{Y}^{\mathbf{n}} + \mathbf{T}_{\boldsymbol{\eta}}\mathbf{x}^{\mathbf{n}}] + \mathbf{B}\ \mathbf{u}^{\mathbf{n}} - \mathbf{T}_{\mathbf{n}}\mathbf{x}^{\mathbf{n}+1} \tag{26}$$

Transforming both sides by $\mathbf{f}_{\mathbf{y}}$ yields, after using the property (16) and (18),

$$\mathbf{Y}_{\mathbf{y}}^{\mathbf{n}+1} = \mathbf{A}_{\mathbf{ta}}\mathbf{Y}_{\mathbf{y}}^{\mathbf{n}} + \mathbf{A}_{\mathbf{ta}}\mathbf{T}_{\eta}\mathbf{x}^{\mathbf{n}} \tag{27}$$

Where

$$\mathbf{A}_{\mathbf{ta}} \equiv (\mathbf{I} - \mathbf{T}_{\eta}\mathbf{T}_{\zeta})\mathbf{A}_{\mathbf{t}} \tag{28}$$

The equation (27) is a system realization of the underlying unsteady aerodynamics. Note carefully that the aerodynamic sub-states $\mathbf{Y}_{\mathrm{y}}$ is generated by the structural states x but there is no other source of excitation for the flow field, which is how the unsteady fluid dynamic equation is governed by the notion of the lifting surface in the case of the small amplitude, dynamically linearized sense. Note that $\mathbf{A}_{\mathrm{ta}}$ is singular because the transformation $\mathbf{I} - \mathbf{T}_{\eta}\mathbf{T}_{\zeta}$ is a singular matrix. Using (7) and (12), the equation (27) can be rewritten in a more compact form,

$$\mathbf{Y}_{\mathbf{y}}^{\mathbf{n}+1} = \mathbf{A}_{\mathbf{ta}}\mathbf{Y}^{\mathbf{n}} \tag{29}$$

It simply states, "The aerodynamic sub-matrix transforms the aeroelastic states at current time step into the aerodynamic sub-states at the next step."

The corresponding aerodynamic force is found by subtracting the input force from the sum of the inertia, damping, and elastic forces according to the D'Alembert's principle:

$$\mathbf{F}^{\mathbf{n}} = \mathbf{x}^{\mathbf{n}+1} - \mathbf{A}\mathbf{x}^{\mathbf{n}} - \mathbf{B}\mathbf{u}^{\mathbf{n}} \tag{30}$$

$$= \mathbf{T}_{\zeta}\mathbf{A}_{\mathbf{t}}\mathbf{Y}_{\mathbf{y}}^{\mathbf{n}} + (\mathbf{T}_{\zeta}\mathbf{A}_{\mathbf{t}}\mathbf{T}_{\eta} - \mathbf{A})\mathbf{x}^{\mathbf{n}} = \mathbf{C}_{\mathbf{ta}}\mathbf{Y}^{\mathbf{n}} - \mathbf{A}\mathbf{x}^{\mathbf{n}} \tag{31}$$

With the aerodynamic output sub-matrix $\mathbf{C}_{\mathrm{ta}}$ is defines as

$$\mathbf{C}_{\mathbf{ta}} \equiv \mathbf{T}_{\zeta}\mathbf{A}_{\mathbf{t}} \tag{32}$$

F is given of the mathematical states **x** that define the structural model, it is desirable to convert **x** to the physical coordinates **w** using (20). In this case, the identified aerodynamics can be easily put into the state-space form by a standard system identification method using **z** as the only driving input to the flow field:

$$\mathbf{y}^{\mathbf{n}+1} = \mathbf{A}_{\mathbf{a}}\mathbf{y}^{\mathbf{n}} + \mathbf{B}_{\mathbf{a}}\mathbf{z}^{\mathbf{n}} \tag{33}$$

$$\mathbf{F}^{\mathbf{n}} = \mathbf{q}(\mathbf{C}_{\mathbf{a}}\mathbf{y}^{\mathbf{n}} + \mathbf{D}_{\mathbf{a}}\mathbf{z}^{\mathbf{n}}) \tag{34}$$

Where **y** is the new aerodynamic states and $q \equiv \frac{1}{2}\rho V^2$ is the dynamic pressure. If **z** represents the modal coordinates vector **p**, **F** becomes the GAF in the traditional sense.

There exists an alternative way to get $\mathbf{A}_{\mathrm{ta}}$ without executing the system identification using (28) and the time history samples **Y** at t=0, Δt , $2\Delta t$,…, $M\Delta t$

$$\mathbf{A}_{\mathbf{ta}} \cong (\mathbf{I} - \mathbf{T}_{\eta}\mathbf{T}_{\zeta})\left[\mathbf{Y}^{1}\ \mathbf{Y}^{2}\ \ldots\ \mathbf{Y}^{\mathbf{M}}\right]\left[\mathbf{Y}^{0}\ \mathbf{Y}^{1}\ \ldots\ \mathbf{Y}^{\mathbf{M}-1}\right]^{-\mathbf{p}} \tag{35}$$

Likewise, $\mathbf{C}_{\mathrm{ta}}$ can be also estimated from the sampled data:

$$\mathbf{C}_{\mathbf{ta}} \cong < \left[\mathbf{F}^{0}\ \mathbf{F}^{1}\ \ldots\ \mathbf{F}^{\mathbf{M}-1}\right] + \mathbf{A}\left[\mathbf{x}^{0}\ \mathbf{x}^{1}\ \ldots\ \mathbf{x}^{\mathbf{M}-1}\right] > \tag{36}$$

Finally, it can be shown that the aeroelastic system matrix is

related to $\mathbf{A}_{ta}$ and $\mathbf{C}_{ta}$ as

$$\mathbf{A}_t = \mathbf{A}_{ta}\ \mathbf{T}_\eta \mathbf{C}_{ta} \tag{37}$$

F. Reduced-Order Aeroelastic Model

Coupled aeroelastic equations of motion can be obtained by coupling the identified aerodynamic system (26), (31), with the structural dynamic (19), (20). After rescaling (31) by the reference dynamic pressure we obtain the following aeroelastic ROM:

$$\begin{Bmatrix} \mathbf{Y}_\mathbf{n}^{\mathbf{n+1}} \\ \mathbf{x}^{\mathbf{n+1}} \end{Bmatrix} = \begin{bmatrix} \mathbf{A_{ta}} & \mathbf{A_{ta}T}_\eta \\ \mathbf{qC_{ta}} & \mathbf{A} + \mathbf{q(C_{ta}T}_\eta - \mathbf{A}) \end{bmatrix} \begin{bmatrix} \mathbf{Y}_\mathbf{n}^{\mathbf{n}} \\ \mathbf{x}^{\mathbf{n}} \end{bmatrix} + \begin{bmatrix} 0 \\ \mathbf{B} \end{bmatrix} \mathbf{u}^{\mathbf{n}} \tag{38}$$

Or, if we use (33) and (34) instead,

$$\begin{Bmatrix} \mathbf{y}_\mathbf{n}^{\mathbf{n+1}} \\ \mathbf{w}^{\mathbf{n+1}} \end{Bmatrix} = \begin{bmatrix} \mathbf{A_a} & [\mathbf{B_a}\ 0] \\ \mathbf{qC_a} & \mathbf{A} + \mathbf{q}[\mathbf{D_a}\ 0] \end{bmatrix} \begin{Bmatrix} \mathbf{y}^{\mathbf{n}} \\ \mathbf{w}^{\mathbf{n}} \end{Bmatrix} + \begin{bmatrix} 0 \\ \mathbf{B} \end{bmatrix} \mathbf{u}^{\mathbf{n}} \tag{39}$$

It should be mentioned that when w is given in terms of the modal coordinates p, (39) becomes valid for any combinations of the air density and airspeed, (ρ, V), making it possible to use the model for different altitudes with the Mach number fixed, in this case, one must allow the time step dt to vary as a function of the airspeed according to $\Delta t = {}^{V_{ref}}\!/_{V}\, \Delta t_{ref}$. However, this is not feasible using (38) because the structural states vector x was defined for the reference time frame in which the time samples were taken. That is, the aeroelastic system defined by (38) works only for the fixed airspeed, ${}^{V_{ref}}\!/_{V}$, with the dynamic pressure allowed to vary through variation in the air density only.

$$\begin{Bmatrix} \mathbf{Y}_y^{\mathbf{n+1}} \\ \mathbf{x}^{\mathbf{n+1}} \end{Bmatrix} = \begin{bmatrix} \mathbf{A_{ta}} & \left[\left(\mathbf{A_{ta}T}_\eta \right)_d \dfrac{V_{ref}}{V} \left(\mathbf{A_{ta}T}_\eta \right)_v \right] \\ q\mathbf{C_{ta}} & \mathbf{A} + q \left[\left(\mathbf{C_{ta}T}_\eta - \mathbf{A} \right)_\mathbf{d} \dfrac{V_{ref}}{V} \left(\mathbf{C_{ta}T}_\eta - \mathbf{A} \right)_\mathbf{v} \right] \end{bmatrix} \begin{bmatrix} \mathbf{Y}_\mathbf{y}^{\mathbf{n}} \\ \mathbf{x}^{\mathbf{n}} \end{bmatrix} + \begin{bmatrix} 0 \\ \mathbf{B} \end{bmatrix} \mathbf{u}^{\mathbf{n}} \tag{40}$$

Where the subscripts d and v refer to the first and second half of the structural coordinates corresponding to the displacements and velocities, respectively.

With this modification, both the aeroelastic system (39) and (40) are valid for all dynamic pressure values at the fixed Mach number and hence can be used for CMVD analyses, e.g., flutter prediction, dynamic loads, and control system design. For example, taking logarithm of the eigenvalues of the system matrix yields aeroelastic roots in the continuous-time domain and hence will determine the stability of the aeroelastic system.

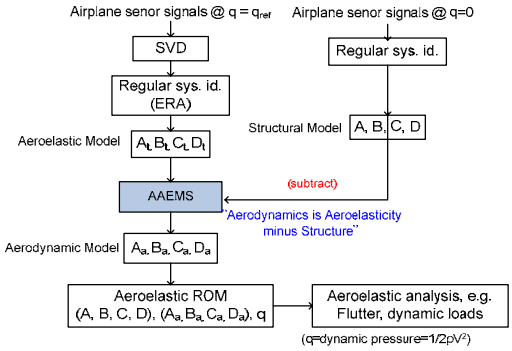

Fig. 1 Flow chart for the AAEMS system identification

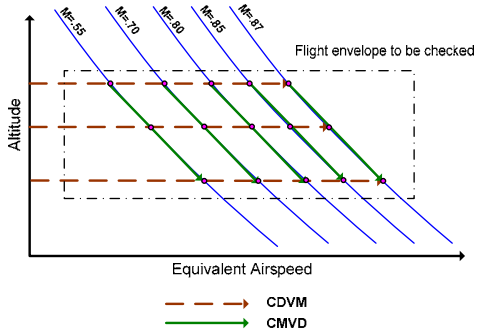

Fig. 2 Comparison of CDMV and CMVD method

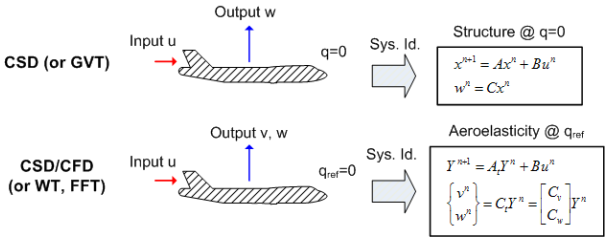

Fig. 3 Regular system identification of structural and aeroelastic systems

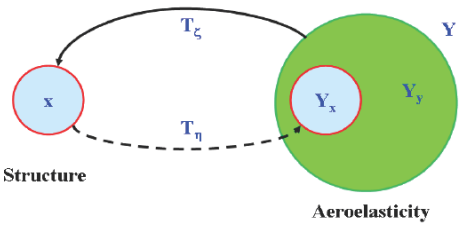

x = structural states (R x 1)
Y = aeroelastic states (R_t x 1) (R_t > R)
Y_x = structural sub-states (R_t x 1)
Y_y = aerodynamic sub-states (R_t x 1)

Fig. 4 Topology and transformation of states

III. RESULTS AND DISCUSSION

A. Aeroelastic Analysis on Reference Dynamic Pressure

The AGARD 445.6 wing is one of the most frequently used benchmarks in aeroelasticity study. The wing model has a panel

aspect ratio of 4.0, a taper ratio of 0.6, a quarter-chord sweep of 45°, and a NACA 64A004 aerofoil section. The semi-span of this model is 0.762 m and the root chord is 0.559 m (see Fig. 5).

For aeroelastic simulations, structural finite element model for AGARD 445.6 wing model is constructed as using solid hex element (see Fig.6). The total number of structural nodes is 609. Materials of the wing structure model are presented in Table I. The root section is clamped to impose structural boundary condition.

Natural frequencies are presented in Fig. 7. The results typically show that the 1st Eigen mode is the fundamental bending mode. The 2nd mode is 1st torsion mode. The 3rd mode is a kind of 2nd bending mode. The 4th mode corresponds to 2nd torsion mode. The pressure data at standard dynamic pressure should be extracted for the analysis of ROM. Wind tunnel test or CSD/CFD analyses are conducted for that. In this study, the pressure data is extracted using fluid-structure coupling algorithms. Fluid-structure coupling algorithm and main integration code including required various sub-modules have been successfully developed in this study. Practical program module (FSIPRO3D Ver.1.0) developed by CAE-KOREA Inc. can be applied to general fluid-structure interaction problems. FSIPRO3D can effectively combine FLUENT software and any kind of commercial finite element software such as SAMCEF, MSC/NASTRAN, ABAQUS, and ANSYS etc. for the general applications of FSI problems. Fig. 8 shows the system process for FSIPRO3D program.

Fig. 9 shows computational grid for AGARD 445.6 wing model. The total element number of the surface grid is 7,286 and that of the domain grid is 24,321. Flow conditions for certification of ROM are 0 degree angle of attack with Mach 0.596, 0.678, 0.96 and 1.14.

The process of aeroelastic analysis is that dynamic aeroelastic analysis is conducted after static analysis is conducted. Damping ratio is assumed as 0.95 in case of static aeroelastic analysis and is assumed as 0.01 in case of dynamic aeroelastic analysis. The altitude of dynamic pressure is defined by the equation below

$$q_f = \frac{1}{2}\rho_\infty \upsilon^2 = \frac{1}{2}\gamma P_\infty M_\infty^2 \tag{41}$$

The spec of computing system is Intel Core2 Quad 2.66 Hz CPU with 4 GB RAM. The time step of 0.0005 sec and the imposed number of subiterations is 20.

B.Aeroelastic Analysis Using Reduced-Order Model

Aeroelastic Analysis Using Reduced-Order Model

When aeroelastic response data and structural data are prepared, Condition matrix of aerodynamic model; Aa, Ba, Ca and Da can be calculated using those data. Aeroelasitc ROM can be developed from the condition matrix. MATLAB (Ver. 7.0) supplying numerical simulation and programming algorithm is used for this process.

Figs. 10~11 represent eigenvalue for reduced-order aeroelastic model at standard dynamic pressure and flutter dynamic pressure with Mach 0.596 and eigenvalue for reduced-order aeroelastic model developed from ERA and AAEMS. Fig. 11 shows the eigenvalue at standard dynamic pressure ratio (q=1) and the eigenvalue at 138% of dynamic pressure ratio. The analyses at Mach 0.678, 0.96 and 1.14 are conducted using the same method. Using the pressure, velocity and displacement data from the analyses, aeroelastic ROM is developed and then flutter boundary is predicted from the ROM analysis. Fig. 12 shows modal displacement and modal velocity according to initial condition at Mach 0.596. Fig. 13 shows eigenvalue calculated using aeroelastic ROM according to various Mach number.

Table II and Fig. 14 represent the comparison results for flutter boundaries for the AGARD 445.6 wing between experimental data and computational results. It is shown that the results from aeroelastic ROM have a good correlation with full-simulation results. It's because the sample values used for ROM analyses were calculated from full-simulation analysis.

TABLE I
MATERIAL PROPERTIES OF AGARD 445.6 WING

Elastic Modulus	E11 = 3.15 GPa
Elastic Modulus	E22 = 0.4162 GPa
Shear Modulus	E12 = 0.4392 GPa
Poisson's Ratio	0.31
Density	393.5 kg/m^3

TABLE II
FLUTTER BOUNDARIES DYNAMIC PRESSURE FOR THE AGARD 445.6 WING

	M 0.596	M 0.678	M 0.96	M 1.14
Experiment	6000 Pa	5540 Pa	2927 Pa	5047 Pa
ROM	5959 Pa	5502 Pa	2450 Pa	6056 Pa
Full-simulation	5850 Pa	5380 Pa	2550 Pa	5715 Pa

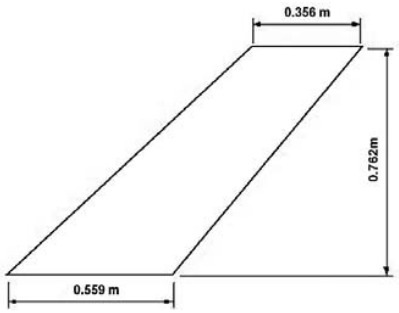

Fig. 5 Geometric configuration of AGARD 445.6 wing

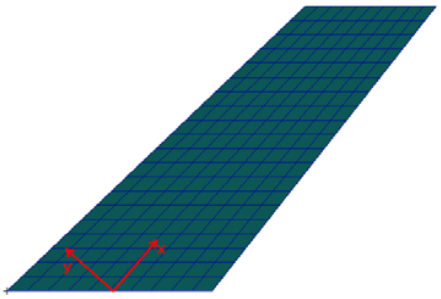

Fig. 6 Finite element model of AGARD 445.6 wing

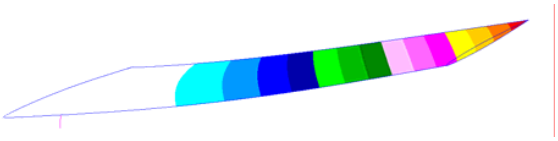

(a) Mode 1 (1st bending, 9.61 Hz)

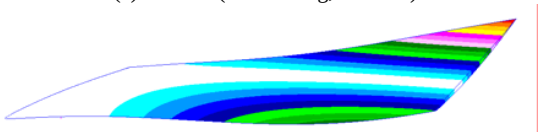

(b) Mode 2 (1st torsion, 38.98 Hz)

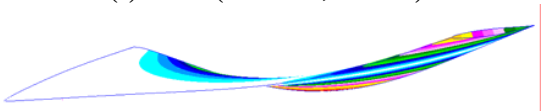

(c) Mode 3 (2nd bending, 48.96 Hz)

(d) Mode 4 (2nd torsion, 93.50 Hz)

Fig. 7 Natural frequency mode shape on FEM grid

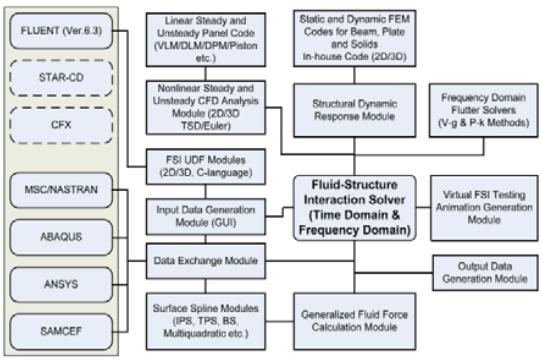

Fig. 8 FSI-PRO 3D System configuration

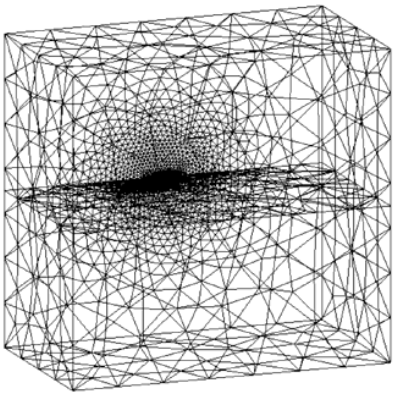

(a) Computational domain grid

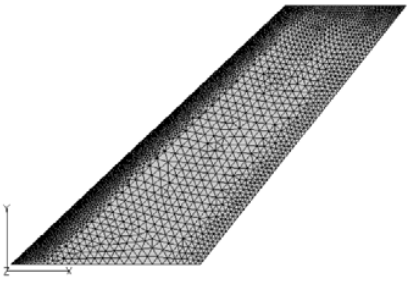

(b) Computational surface grid

Fig. 9 Computational grid for AGARD 445.6 wing model

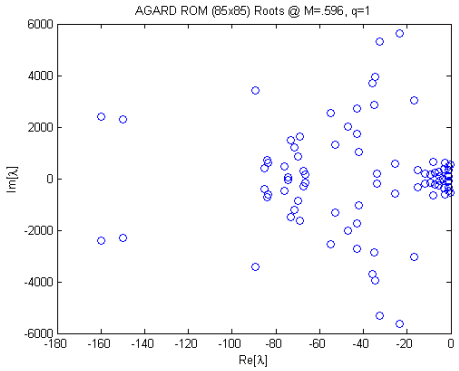

Fig. 10 Eigenvalues of the aeroelastic ROM identified by ERA and AAEMS

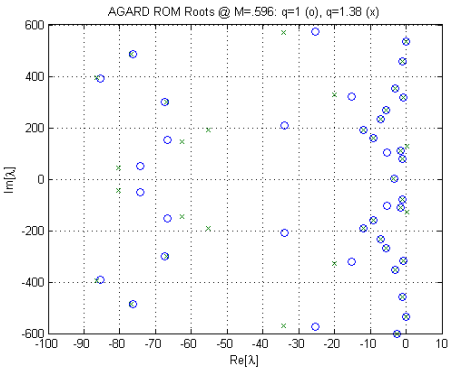

Fig. 11 Eigenvalues of the aeroelastic ROM at two dynamic pressures (q=1.0, 1=1.38)

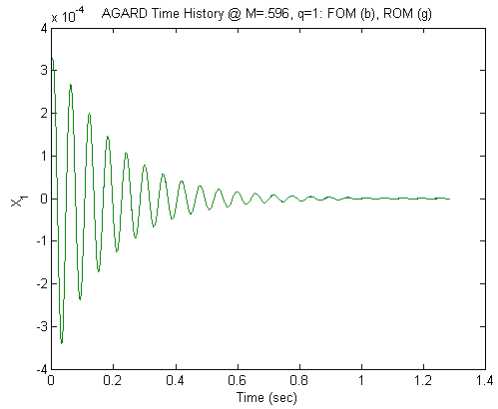

(a) 1st mode displacement

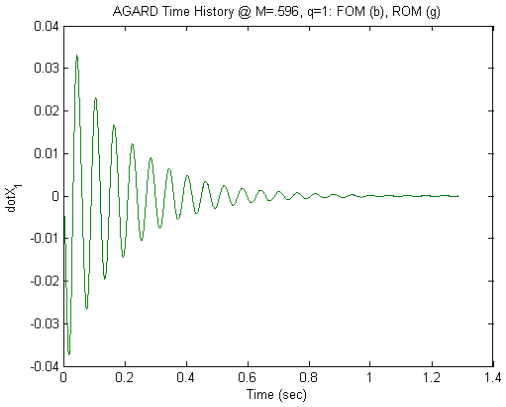

(b) 1st mode velocity

Fig. 12 Aeroelastic response due to initial condition

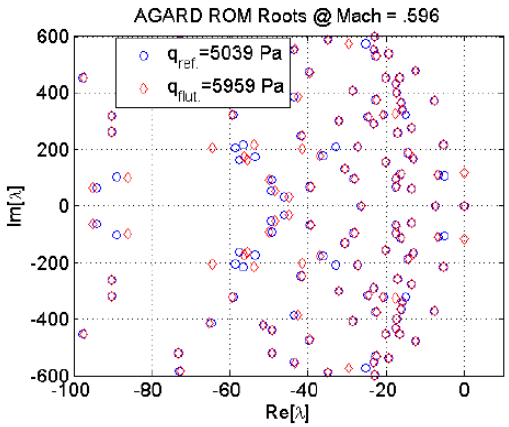

(a) Mach 0.596

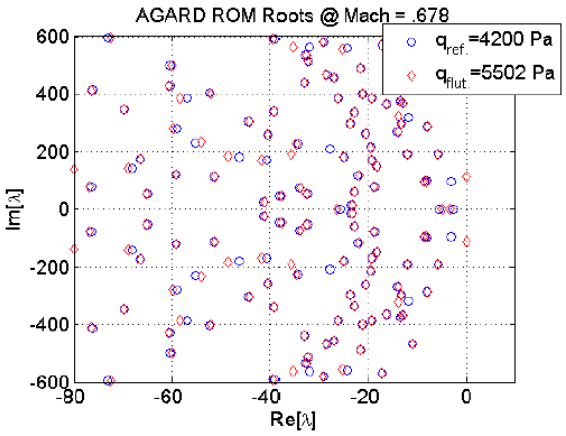

(b) Mach 0.678

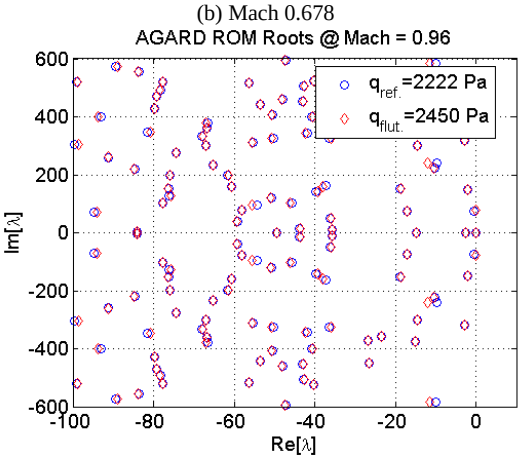

(c) Mach 0.96

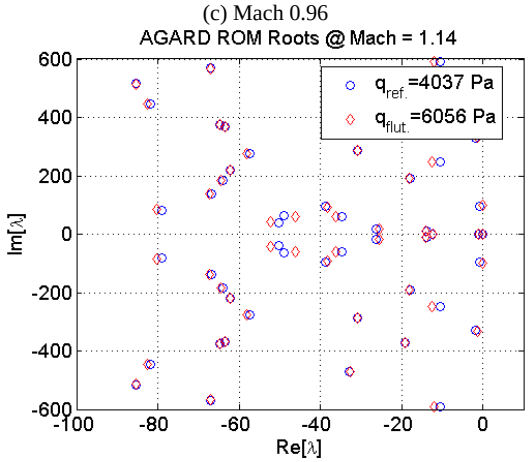

(d) Mach 1.14

Fig. 13 Eigenvalues on AGARD 445.6 wing ROM roots

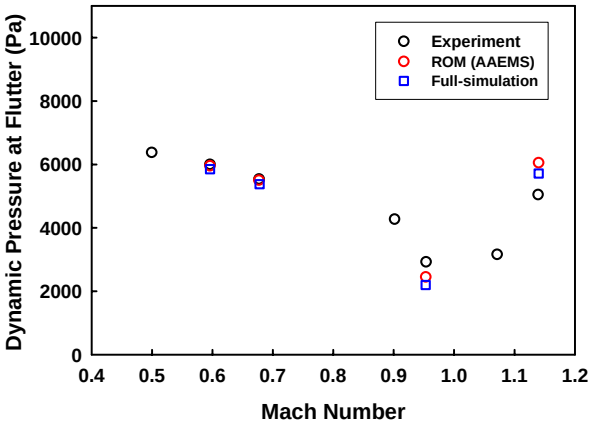

Fig. 14 Flutter boundaries for the AGARD 445.6 wing

IV. CONCLUSION

In this study, Reduced-Order aeroelastic model is successfully developed using AAEMS method and then flutter boundaries at subsonic, transonic and supersonic region for the AGARD 445.6 wing is predicted by the process. The analysis of fluid-structure interaction is conducted using CFD method for calculating aeroelastic response data at standard dynamic pressure. Reduced-Order aeroelastic model is successfully developed with ERA and AAEMS method using aeroelasitc response data. The flutter boundaries calculated from ROM method is compared to experiment data and full-simulation result. It is shown that the results from ROM method have a good correlation with full-simulation results. Although it has long time to develop Reduced-Order aeroelastic model, the computing time for predicting flutter boundary is very fast. The ROM method is good for calculating dynamic force, optimization and design of a closed circuit control system as well as predicting flutter boundary.

ACKNOWLEDGMENT

This work was partially supported by Defense Acquisition Program Administration and Agency for Defense Development under the contract (UD070041AD) and DRC (Degree and Research Center) program.

REFERENCES

[1] K. C. Hall, "Eigenanalysis of Unsteady Flows About Airfoil, Cascades, and Wing," AIAA Journal, Vol. 32, No. 12, 1994, pp. 2426-2432.
[2] E. H. Dowell, K. C. Hall, and M. C. Romanowski, "Eigenmode Analysis in Unsteady Aerodynamics; Reduced-Order Models," Applied Mechanics Review, Vol. 50, No. 6, 1997, pp. 371-386.
[3] M. C. Romanoski, "Reduced-Order Unsteady Aerodunamic and Aeroelastic Models Using Karhunen-Loeve Eigenmodes," AIAA-96-3981, AIAA Symp. On Multidisciplinary Anal. And Optim., Bellevue, WA.
[4] T. Kim, "Frequency-Domain Karhunen-Loeve Method and Its Application to Linear dynamic Systems," AIAA Journal, Vol.36, No. 11, 1998, pp. 2117-2123.
[5] K. Hall, J. P. Thomas, and E. Dowell, "Proper Orthogonal Decomposition Technique for Transonic Unsteady Aerodynamic Flows," AIAA Journal, Vol. 38, No. 10, 2000, pp. 1853-1862.
[6] T. Kim, and J. E. Bussoletti, "An Optimal Reduced-Order Aeroelastic Modeling Based on a Response-Based Modal Analysis of Unsteady CFD Models," AIAA-2001-1525, 42nd AIAA/ASME/ASCE/AHS/ASC Structures, Structural Dynamics, and Materials conference, Seattle, WA, April 2001.
[7] W. A. Silva, "Application of Nonlinear Systems Theory to Transonic Unsteady Aerodynamic Responses," Journal of Aircraft, Vol. 30, No. 5, 1993, pp. 660-668.
[8] D. E. Raveh, "Identification of Computational Fluid Dynamic Based Unsteady Aerodynamic Models for Aeroelastic Analysis," Journal of Aircraft, Vol. 41, No. 3, 2004, pp. 620-632.
[9] T. Kim, M. Hong, K. G. Bhatia, and G. Sengupta, "Aeroelastic Model Reduction for Affordable Computational Fluid Dynamics-Based Flutter Analysis," AIAA Journal, Vol. 43, No. 12, 2005, pp. 2487-2495.
[10] K. K. Gupta, and C. Bach, "Systems Identification Approach for a Computational-Fluid-dynamics Based Aeroelastic Analysis," AIAA Journal, Vol. 45, No. 12, 2007, pp. 2820-2827.
[11] Kim, T., "New System Identification for Coupled Fluid-Structure Systems: Aerodynamics is Aeroelasticity minus Structure," IFASD-2009-073, International Forum on Aeroelasticity and Structural Dynamics, Seattle, WA, June 2009.
[12] Kim, T., "System Identification for Coupled Fluid-Structures: Aerodynamics is Aeroelasticity minus Structure," AIAA Journal, Volume 49, No. 3, 2011, pp. 503-512.